Epoxy-Based Carbon Fiber-Reinforced Plastics Recycling via Solvolysis with Non-Oxidizing Methanesulfonic Acid

Xiaohui Zhang, Reda Sibari, Souvik Chakraborty[§], Stephan Baz, Götz T. Gresser, Wladislaw Benner, Thilo Brämer, Leif Steuernagel, Emanuel Ionescu, Joachim Deubener, Sabine Beuermann, Gerhard Ziegmann* and René Wilhelm*

DOI: 10.1002/cite.202300243

The urgent requirement for efficient recycling strategies in the wind energy industry prompted this study to explore the behavior of methanesulfonic acid (MSA) in the solvolysis of carbon fiber-reinforced plastics (CFRP), as an alternative to standard solvents and acids. For the investigation, two layers of carbon fibers, infused with amine-based epoxy through a vacuum-assisted resin infusion process, were applied. The results showed that MSA was the most effective solvent for the solvolysis of CFRP, compared to other investigated common acids. The recycled products demonstrated satisfactory properties for both the matrix and fiber, which were comparable to those of the virgin materials.

Keywords: Carbon fibers, Epoxy resin, Recycling, Solvolysis

Received: December 21, 2023; *revised:* April 22, 2024; *accepted:* April 24, 2024

1 Introduction

The extensive release of end-of-life wind turbine blade materials into the environment has given rise to a significant ecological crisis [1–3]. The complex nature of these blades, primarily composed of epoxy resin, glass, and carbon fibers (CF), presents challenges in terms of their recyclability [4–7]. Unlike thermoplastic composites, which can undergo melting and reprocessing into new forms, the presence of a heavily crosslinked structure in the matrices of these wind turbine blades often hinders efficient matrix and fiber recovery, resulting in downsizing [8–10].

Disposal routes such as incineration and landfilling are available [11–13]; however, they face increasing restrictions in Europe due to environmental protection laws [14–16]. Addressing the recycling challenge of CF-reinforced plastics (CFRP), three common recovery routes are considered: energy recovery, physical recovery, and chemical recovery [17–20]. Recent studies have focused on investigating milder chemical recovery methods for CFRP under atmospheric pressure conditions [21–23].

Yet, degradation systems employing nitric acid [24, 25] and benzyl alcohol with tripotassium phosphate [26, 27] have drawbacks, such as strong oxidizing conditions or the generation of undesirable by-products during the reaction. Furthermore, the approach of utilizing less problematic substances, such as water [28–31] and alcohols like methanol [32] and propanol [33, 34] in their supercritical states, necessitates stringent conditions, including elevated temperatures and high pressures, which are notably energy intensive. An alternative two-step method involving solvent penetration followed by decomposition with oxidants has been explored

[1,2]Xiaohui Zhang, [1,2]Reda Sibari, [1]Souvik Chakraborty, [3]Stephan Baz, [3]Götz T. Gresser, [4]Wladislaw Benner, [4]Thilo Brämer, [1]Dr. Leif Steuernagel, [4]Emanuel Ionescu, [5]Joachim Deubener, [6]Sabine Beuermann, [1]Gerhard Ziegmann (ziegmann@tu-clausthal.de), [2]Prof. René Wilhelm https://orcid.org/0000-0003-3856-2757 (rene.wilhelm@tu-clausthal.de)

[1]Institute for Polymer Materials and Plastics Engineering, Clausthal University of Technology, Agricolastr. 6, 38678 Clausthal-Zellerfeld, Germany.

[2]Institute of Organic Chemistry, Clausthal University of Technology, Leibnizstr. 6, 38678 Clausthal-Zellerfeld, Germany.

[3]German Institutes of Textile and Fiber Research Denkendorf, Koerschtalstr. 26, 73770 Denkendorf, Germany.

[4]Fraunhofer Research Institution for Materials Recycling and Resource Strategies IWKS, Brentanostr. 2a, 63755 Alzenau, Germany.

[5]Institute of Non-Metallic Materials, Clausthal University of Technology, Zehntnerstraße 2A, 38678 Clausthal-Zellerfeld, Germany.

[6]Institute of Technical Chemistry, Clausthal University of Technology, Arnold-Sommerfeld-Straße 4, 38678 Clausthal-Zellerfeld, Germany.

[§]Present address: Dept. Sustainability Technologies, Institute of Lightweight Systems, German Aerospace Center (DLR), Lilienthalplatz 7, 38108 Braunschweig, Germany.

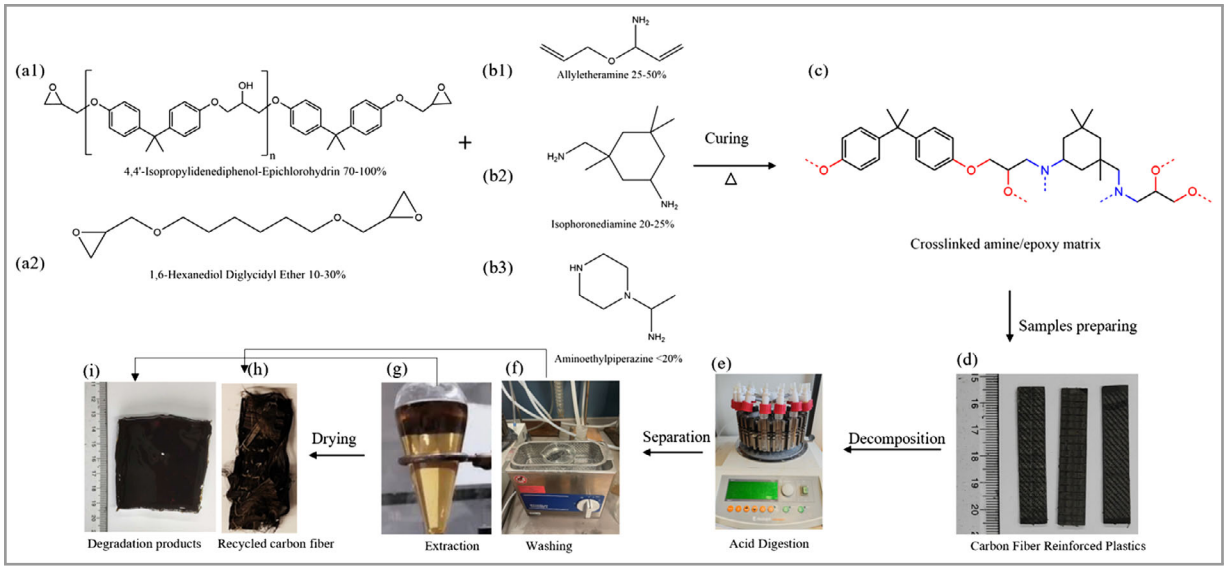

Figure 1. Schematic representation of the recycling process.

[35–37]. However, this approach leads to prolonged reaction times and increased energy costs.

In contrast, methanesulfonic acid (MSA) has emerged as a standout organic acid due to its superior qualities and easy synthesis [38–40], showing promise as an agent for breaking down the resin system and CF coating with minimal damage to the CF, as has been observed during this present work. Furthermore, MSA exhibits environmentally friendly characteristics, including low toxicological risk, high chemical stability, and biodegradability, making it an attractive option for various chemical reactions [41].

In this study, an energy-efficient method is presented for the decomposition of a crosslinked epoxy network by cleaving specific bonds present in amine-cured epoxies under mild conditions (<100 °C) and atmospheric pressure. After comparative analysis, we report that MSA was the most effective solvent, efficiently reclaiming both the carbon and epoxy resin in good quality compared to nitric acid and acetic acid (Sect. 4). The decomposed resin and recovered CF were extensively characterized using Fourier transform infrared (FTIR) spectroscopy, gel permeation chromatography (GPC), differential scanning calorimetry (DSC), thermogravimetric analysis (TGA), Raman spectroscopy, scanning electron microscopy (SEM), and single-fiber testing. Our approach focused on evaluating the efficiency of CF and resin recovery while optimizing recycling parameters to ensure energy and reagent savings.

2 Experimental Section

2.1 Sample Manufacturing and Preparation

The epoxy resin under investigation is the Hexion EPIKOTE^{TM} Resin MGS^{TM} RIMR 135, along with the amine hardener EPIKURE^{TM} Curing Agent MGS^{TM} RIMH 137, which finds widespread commercial use in wind energy and maritime applications. Although the component of the resin system is proprietary and not publicly disclosed, to enhance comprehension of the chemical mechanisms during polymerization, a potential resin component [42] and the corresponding reaction mechanism [43] are illustrated in Fig. 1. The resin component comprises bisphenol A diglycidyl ether (DGEBA) (Fig. 1a1; 70–100 %) and 1,6-hexanediol diglycidyl ether (HDDGE) (Fig. 1a2; 10–30 %). The reactive amines used in the hardener are alkyletheramine (Fig. 1b1; 25–50 %), sophorone diamine (IPDA) (Fig. 1b2; 20–24 %), and aminoethylpiperazine (Fig. 1b3; <20 %).

The formulation of composites intended for subsequent recycling was executed as detailed in a prior investigation [44]. Two layers of bi-directional (0/90) CF layers with a calculated fiber volume fraction (FVC) of approximately 45 % (Tab. 1) were infused with the resin system in a mixing ratio of 100:30 (by weight) using the vacuum-assisted resin infusion (VARI) process [45]. The fabrics were stitched with polyester threads (6 g m^{-2}). The post-curing process was conducted at a temperature of 70 °C for 15 h. Frekote 770NC from Henkel was used as the mold release agent.

Table 1. Characteristics of the CFRP.

CFRP	Value
Number of fiber layers	2
Weight of the fibers [g]	2.645
Area of one layer [m^2]	0.002049
Average thickness of the composites [mm]	1.6
Density of the fibers [g cm^{-3}]	1.8
FVC of the CFRP before dissolving [%]	44.8

2.2 Recycling Process

The CFRP samples utilized in this study had dimensions of 50 mm × 10 mm × 2 mm (Fig. 1d). The recycling reaction was carried out using a liquid phase synthesis system named "Synthesis 1" (Fig. 1e; Heidolph). The specimens were placed inside a 25-mL glass tube with three different acids: MSA (>99.0 %; TCI Deutschland GmbH), acetic acid (>99.9 %; Honeywell Riedel-de Haën™), and nitric acid (>65 %; Honeywell Fluka). The reaction mixture was subjected to shaking at a frequency of 550 rpm for a duration of 0.5–3 h at a temperature of 90 °C. Following the recycling process, the recovered CF were washed with water in an ultrasonic bath (Fig. 1f) until reaching a neutral pH value. Subsequently, the CF were dried in an oven at 200 °C for 24 h. To monitor any weight loss during the recycling process, the weight of the samples was recorded before and after recycling. The decomposition mixture and washing solution of the recycled fibers was neutralized using solid sodium carbonate and then extracted with ethyl acetate, utilizing a separatory funnel (Fig. 1g). The resulting degradation products of the resin were collected for further evaluation by removing the ethyl acetate by rotary evaporation at 40 °C.

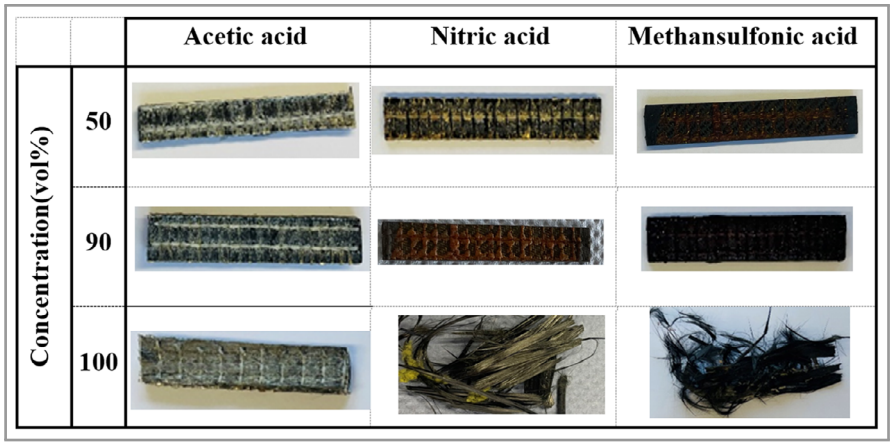

Figure 2. rCF samples after acidic treatment at various concentrations.

2.3 Characterization Techniques

FTIR spectra were acquired using an Alpha T-IR instrument from Bruker, recording the spectra in the frequency range of 400–4000 cm^{-1}. All values were normalized against the peak at 1720 cm^{-1} corresponding to the ester carbonyl group. Raman spectra were obtained with a Horiba HR800 micro-Raman spectrometer (Horiba Jobin Yvon GmbH, Bensheim, Germany), employing an argon laser with a wavelength of 514.5 nm. The excitation line was filtered to exclude plasma emission and a Raman notch filter was used to reject laser light. Measurements utilized a 600-line grating and a confocal microscope (magnification 50×, numerical aperture (NA) = 0.5) with a 100-µm aperture, yielding a resolution of approximately 2–4 µm. The laser power (20 mW) was attenuated with neutral density filters, ensuring that the power on the sample remained below 2 mW. All spectra were background subtracted, smoothed (SMA, simple moving average), and fitted to Lorentzian line shapes. TGA was performed using a TGA 2950 according to DIN EN ISO 11358 to investigate the residual resin on the recovered CF. The temperature was increased from 25 to 500 °C with a ramp of 10 °C min^{-1} under a nitrogen atmosphere to prevent undesired reactions. DSC analyses were conducted in a DSC 2929 calorimeter from TA Instruments under an inert nitrogen (N_2) atmosphere. The analysis followed a heat-cool-heat regime from −20 to 200 °C (heating up to 200 °C at a ramp rate of 10 °C min^{-1}, cooling down to −20 °C at a ramp rate of 50 °C min^{-1}, followed by heating to 200 °C at a ramp rate of 10 °C min^{-1}). T_g (mid-point glass transition) values were obtained from the first run using the TA Universal Analysis software. The surface morphology of the CF was examined using a DSM 982 Gemini scanning electron microscope with an accelerating voltage of 15 kV in the secondary electron (SE) mode. GPC was utilized to determine the molecular weight distribution (MWD) of the recovered epoxy resin. A Waters 515 HPLC pump, a Knauer Marathon Autosampler, a Knauer Smartline refractive index detector 2300, and three SDV separation columns from Polymer Standards Service (PSS; Mainz, Germany) with 100, 1000, and 100 000 Å were employed. 1,1,1,3,3,3-Hexafluoroisopropanol (HFIP) was used as eluent and calibration was established with poly(methyl methacrylate) (PMMA) standards. Single-fiber tensile tests were conducted using a semi-automated single-fiber testing machine (TexTechno, Favimat$^+$) with a fiber length of 50–60 mm. Mechanical response analysis of the CF after different dissolution intervals was performed on 30 fibers tested with a gauge length of 25 mm and a crosshead speed of 5 mm min^{-1}. The fiber cross-sectional area was measured using the built-in vibroscope system.

3 Results and Discussion

3.1 Decomposition of the Composites

To evaluate the efficiency of CF recovery, a visual inspection was performed to examine the recovered fibers. Fig. 2 shows that fibers recovered with acetic acid exhibited good shape retention with only a slight increase in size. However, the acidity of acetic acid was not strong enough to break the polyester stitches, leading to hindered diffusion and

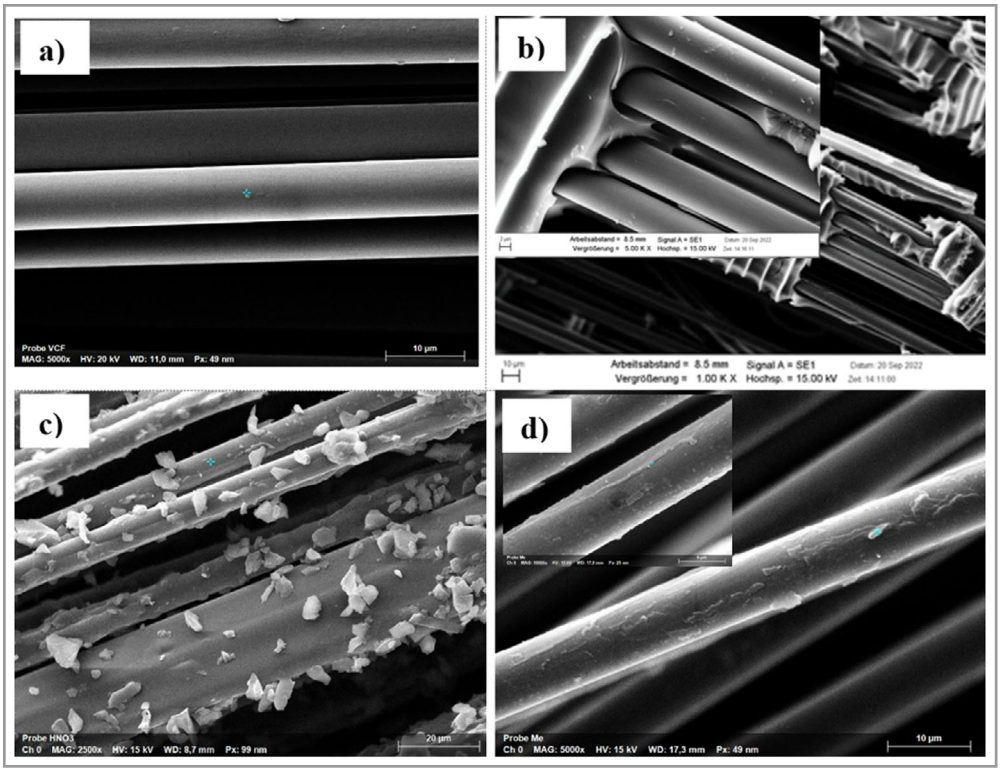

Figure 3. SEM images of the CF: (a) virgin fiber; recovered with (b) acetic acid, (c) nitric acid, and (d) MSA.

prolonged recycling times. In contrast, the use of nitric acid and MSA successfully dissolved the cross-stitches, releasing the fibers from the rigid form of the samples. This allowed for efficient recovery of the CF. The recovered fibers could be further processed into textile preforms, reducing the need for fibers from virgin sources in the composites industry.

To assess the characteristics of the retrieved fibers, the morphologies of both virgin and recycled fibers were investigated using SEM, as depicted in Fig. 3. The observations revealed that CF recovered with acetic acid (Fig. 3b) or nitric acid (Fig. 3c) exhibited a notable presence of matrix remnants on their surfaces. In case of nitric acid, it is also possible that the outer layers of the CF were oxidized, leaving oxidized fragments on the surface of the remaining fiber. Conversely, the CF recovered using MSA (Fig. 3d) appeared almost devoid of such residual coatings.

To assess the residue on the fibers, the residual matrix on the fibers was calculated using the following formula:

$$\text{Residual matrix on fibers (wt \%)} = (W_{rc} - W_f)/W_m \quad (1)$$

where W_{rc} represents the weight of the composites after decomposition/solvolysis and W_f and W_m denote the masses of the CF and the matrix before decomposition (calculated as described before).

The recovery efficiency of the matrix was also determined to gauge the potential reuse of the recovered epoxy resin in future applications. This was calculated by comparing the mass of the recovered matrix (W_{rm}) to the mass of the resin before decomposition (W_m).

$$\text{Recovered matrix (wt \%)} = W_{rm}/W_m \quad (2)$$

Fig. 4 illustrates the outcomes of the calculations from Tab. 2. Notably, when using MSA as the recycling solvent, the residual epoxy resin on the CF surface was the lowest, at 5 %. Simultaneously, the percentage of the recovered matrix was the highest, reaching 89 %, surpassing the outcome obtained using the other two solvents. Conversely, the use of nitric acid resulted in the lowest amount of recovered matrix. This can be attributed primarily to its potent oxidizing properties, which necessitated a higher number of washing cycles during the collection of decomposed resin, ultimately reducing the quantity of the recovered resin.

Due to the superior performance observed with MSA as the recycling solvent, a more detailed investigation into the chemical changes of the recovered epoxy resin was conducted using FTIR spectroscopy. In the FTIR spectra of the recycled materials (Fig. 5), specific absorption bands at 1600, 1494, and 1455 cm^{-1} correspond to the stretching vibration of benzene rings (Tab. 3), indicating preservation of the intact benzene ring structure of the recycled material. Additionally, the intensity of the band at 1240 cm^{-1}, which is assigned to aromatic ethers (C—O—C) in the epoxy resin material, remained relatively unchanged after recycling (Fig. 5). This preservation of the C—O—C bond in aromatic ethers indicates the retention of the essential structural elements during the degradation process. Moreover, the FTIR analysis revealed noteworthy changes in certain

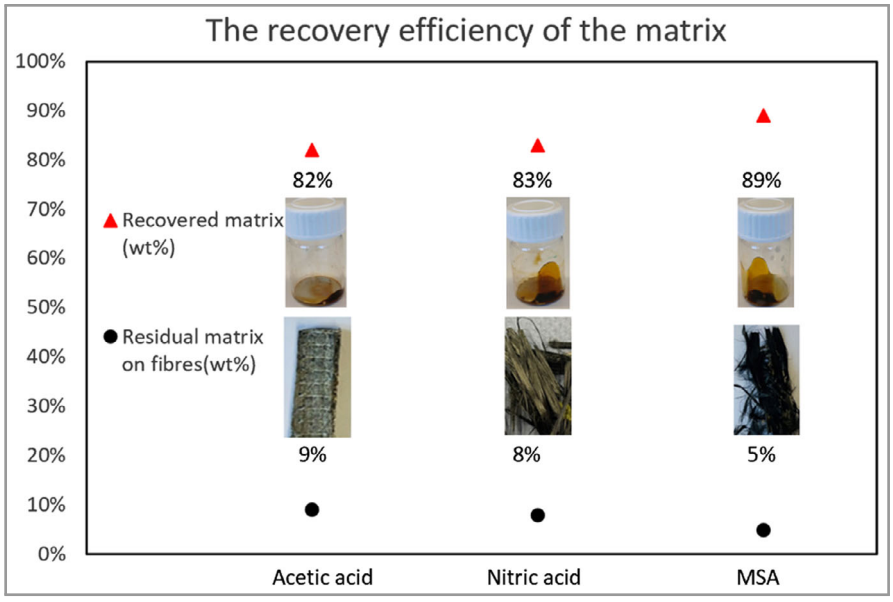

Figure 4. Changes in quantity of residual and recovered matrix on the fibers, with pictorial representation.

bonds. Specifically, there was a reduction in the intensity of the band around 1172 cm^{-1}, corresponding to the C—N stretch bond, indicating the anticipated cleavage of C—N bonds in the recycled epoxy resin (Fig. 5). Simultaneously, there was an increase in the intensity of the band around 3322 cm^{-1}, associated with N—H bonds, further confirming the occurrence of C—N bond cleavage during the recycling process (Fig. 5).

TGA, as depicted in Fig. 6a and summarized in Tab. 4, reveals notable differences between the recycled epoxy resin and the virgin epoxy. Specifically, the recycled epoxy resin exhibits an earlier onset of degeneration, as indicated by the temperature at which a mass loss of 5 wt % occurs (196 °C), compared to the virgin epoxy (306 °C). This early onset can be attributed to a significant reduction in molar mass after decomposition, leading to a more readily degradable structure. However, as the decomposition progresses and reaches 50 wt % mass loss, the difference in temperature between the recycled and virgin epoxy reduces to 34 °C. This suggests that the reduction in molar mass becomes less pronounced at later stages of the decomposition. In conclusion, the thermal properties of the recycled epoxy resin indicate a substantial reduction in its stability and degradation temperature, suggesting that the original epoxy polymer chain undergoes decomposition into shorter components with likely reduced molecular weight.

To further evaluate the structural characteristics, we conducted DSC on samples from both the virgin epoxy and the recovered matrix (Fig. 6b and Tab. 4). T_g was found to decrease significantly from 93 to 43 °C in the recycled epoxy resin. This reduction in T_g can be attributed to an increased mobility of polymer chains, supporting the previous inference of sufficient chemical depolymerization of the heavily crosslinked epoxy network during the solvolysis process.

Table 2. Changes in quantity of residual and recovered matrix on the fibers.

	CFRP-Acetic	CFRP-Nitric	CFRP-MSA
Average thickness [mm]	1.40	1.38	1.37
Average width [mm]	9.27	8.97	10.12
Average length [mm]	35.42	34.85	44.60
Average volume [cm^3]	0.460	0.430	0.617
FVC of CFRP before dissolving [%]	44.8	44.8	44.8
Weight of CFRP before dissolving, W_c [g]	1.76	1.88	1.84
Weight of fiber before dissolving, W_f [g]	0.371	0.347	0.498
Weight of matrix before dissolving, W_m [g]	1.389	1.533	1.342
Recovered matrix, W_{rm} [g]	1.139	1.272	1.195
Recovered CFRP, W_{rc} [g]	0.496	0.470	0.565
Residual matrix on fibers [wt %]	9.0	8.0	5.0
Recovered matrix, W_{rm} [wt %]	82.0	83.0	89.0

3.2 Parameter Variation

Given the promising effectiveness of MSA in the CFRP recycling process, we conducted a series of experiments to investigate the impact of varying reaction parameters. The experiments employing MSA were carried out following the same procedure as in the decomposition process. To assess the decomposition efficiency of the composites, we calculated the decomposition degree (D_d) using the following formula:

$$D_d\,(\text{wt}\,\%) = W_l/W_m = (W_c - W_{rc})/W_m \quad (3)$$

Here, W_l represents the weight loss obtained by subtracting the mass of the composites before decomposition (W_c) from the mass of solid residues after decomposition (W_{rc}).

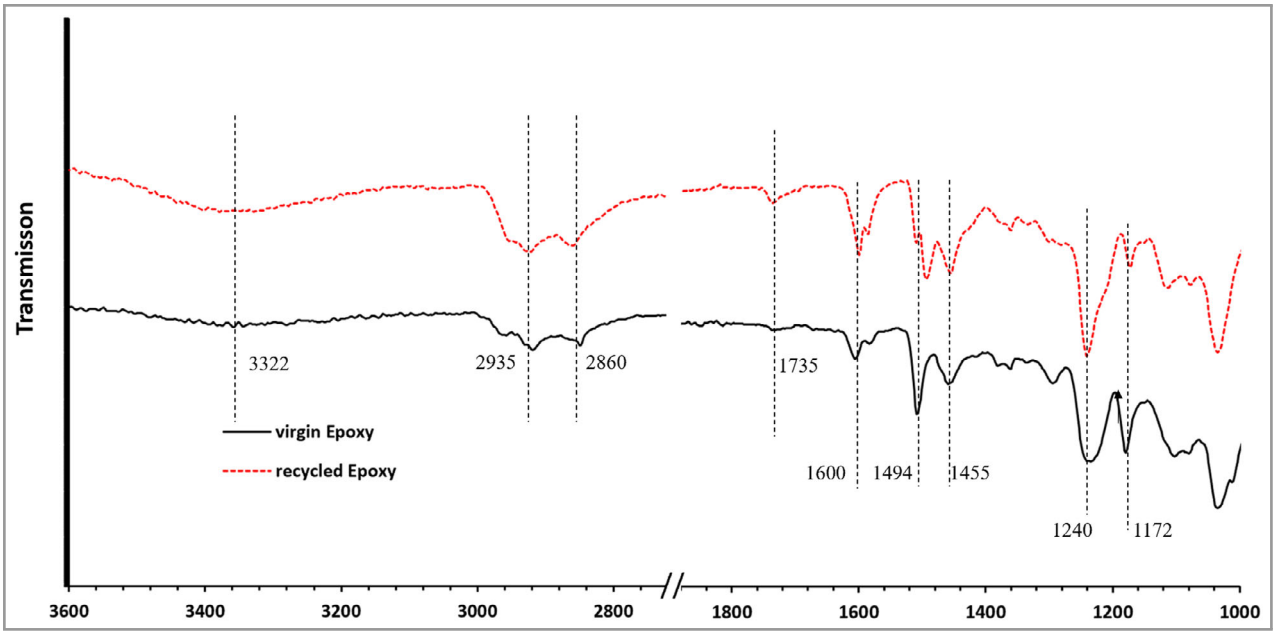

Figure 5. FTIR spectra of the epoxy resin before and after recycling.

W_m signifies the mass of matrix in the composites before decomposition.

Fig. 7 illustrates the results, indicating that some samples exhibit negative decomposition ratios, particularly in solvents mixed with water. This phenomenon could be attributed to the intercalating effect of water molecules between the graphite interlayers of the CF [46]. Moreover, it is evident from the data that the decomposition ratio remains relatively unchanged when the reaction intervals extend beyond 2.5 h with 100 % MSA. This finding suggests that the reaction time is sufficient to achieve the desired outcomes under these conditions.

3.3 Properties of the Recovered Matrix Material

The comparative MWD of the recycled matrix are depicted in Fig. 8, and their respective average molecular weights and dispersities (D) are summarized in Tab. 5. An interesting correlation emerged between the reaction interval and the MWD of the recycled matrix. As the solvolysis time increased, the MWD of the recycled matrix tends to shift towards lower molecular weights. This phenomenon can be attributed to the reduction in chain length resulting from prolonged depolymerization. Furthermore, an extended treatment duration led to a relatively narrow MWD, as evidenced by the reduction in dispersity. It can be postulated that the initial cleavage of amine linker groups resulted in decomposed fragments, followed by gradual shortening of the remaining epoxy chains into repeating units.

Table 3. Characteristic FTIR peaks of epoxy before and after recycling.

Vibration	Virgin epoxy	Recycled epoxy
N—H stretching [cm^{-1}]	3322	3322
C—H stretching [cm^{-1}]	2930, 2860	2935, 2962
C═O [cm^{-1}]	1735	1735
Benzene ring [cm^{-1}]	1600, 1494, 1455	1600, 1494, 1455
C—O—C [cm^{-1}]	1240	1242
C—N [cm^{-1}]	1172	1170

3.4 Properties of the Recycled CF

To assess the impact of the recycling processes on the structural integrity of the fibers, a study was conducted on the mechanical properties of both the virgin and recycled fibers obtained at various reaction intervals (Fig. 9 and Tab. 6). The results indicated that the tensile strength of the recovered fibers, obtained after treating the solution at 90 °C for 2 h, reached 4.0 GPa, representing a reduction of only 13 % (Tab. 6) compared to the value of the virgin CF (4.6 GPa). Additionally, the elongation of the recycled CF (rCF) decreased by only 10.5 %, and the elastic modulus remained virtually unchanged, exhibiting only a 1 % decrease compared to the virgin fibers (Tab. 6). These findings suggest that the performance of the rCF remained relatively unaffected by recycling, as long as the acid exposure time remained less than 2 h. This observation aligns with the conclusions drawn in the parameter changes section, indicating that 2.5 h of solvolysis is a sufficient interval for the desired outcome. However, it is noteworthy

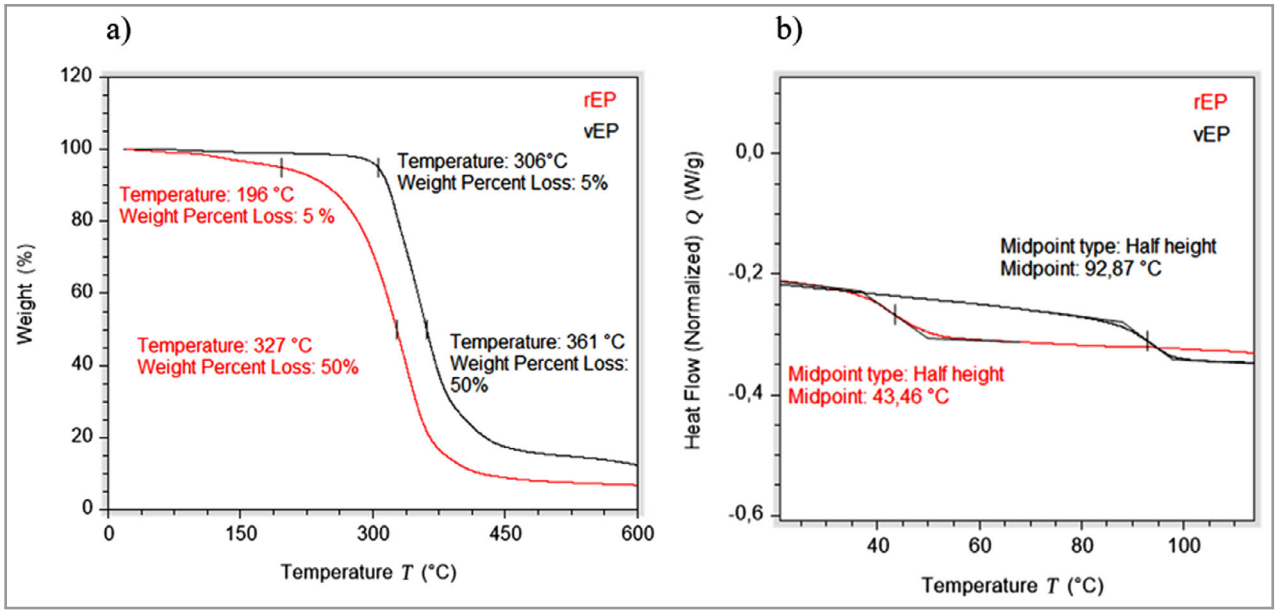

Figure 6. (a) TGA and (b) DSC analysis of recycled epoxy (rEP) and virgin epoxy (vEP).

Table 4. Characteristic threshold from TGA measurements and glass transition from DSC tests.

	95 wt % threshold [°C]	50 wt % threshold [°C]	T_g [°C]
Virgin epoxy	306	361	93
Recycled via MSA	196	327	43
Difference	110	34	50

that the mechanical properties of the rCF experienced some deterioration with prolonged reaction time. Specifically, after 3 h of reaction, there was a 28.3 % reduction in maximal breaking strength and a 19 % decrease in elongation at breakage (Tab. 6). This suggests that an extended solvolysis time may potentially damage the CF, particularly concerning load-bearing capacities. Nevertheless, further investigations in future studies will be conducted to gain deeper insights into this aspect.

To rationalize the effect of solvolysis on the structural properties of the CF as observed above, Raman spectroscopy was used. The Raman spectra of the virgin CF fibers and of the rCF are shown in Fig. 10 and, as expected, indicate the presence of sp^2-hybridized turbostratic carbon. The peak deconvolution of the spectra (shown in Fig. 10) was done using the model of Ferrari and Robertson [47]. The first-order region was deconvoluted with four peaks denoted as T, D, a-C, and G (Fig. 10). The G mode represents the ideal graphitic vibrations (E2g), typical of sp^2-hybridized carbon,

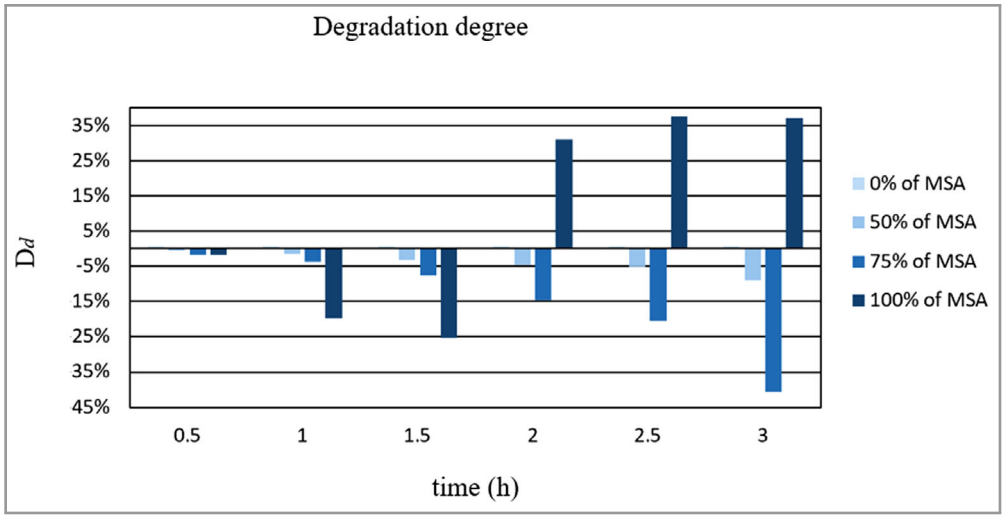

Figure 7. Decomposition ratio with MSA at different concentrations.

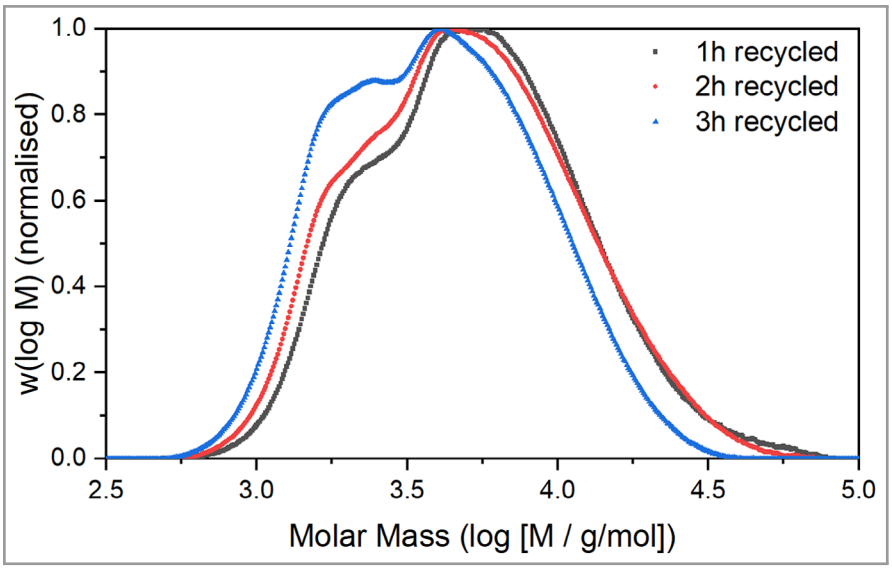

Figure 8. MWD of recycled epoxy resin after different reaction intervals.

Table 5. Number average (M_n) and weight average (M_w) molecular weights and dispersity (D) of recycled epoxy resin after different reaction intervals.

Recycled for	M_n [g mol^{-1}]	% Change M_n to Ref [%]	M_w [g mol^{-1}]	% Change M_w to Ref [%]	D
1 h	3953	0	7401	0	1.87
2 h	3640	−7.9	6937	−6.3	1.91
3 h	3033	−23.3	5323	−28.1	1.76

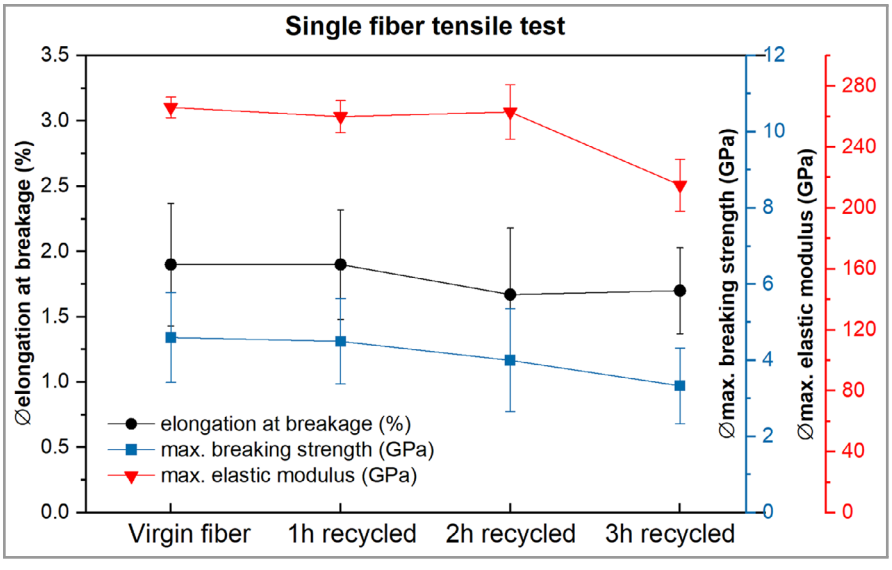

Figure 9. Mechanical properties of virgin and recycled fibers after 1, 2, and 3 h of exposure to solvolysis.

whereas the other modes (T, D, and a-C) correspond to disordered graphitic vibrations. In the second-order region, the spectrum was also fitted with four peaks denoted as D+D″, 2D, D+G, 2D′ [47]. Extensive work was performed in order to attain structural information about the microstructure and quality of carbonaceous materials from the Raman modes mentioned above.

Various parameters were defined within this context, including the lateral cluster size (L_a) [47, 48] and the inter-defect distance (L_D) [49], which give indications about the crystallinity (i.e., crystallinity is larger when L_a is larger) as well as about the defect density (i.e., defect density increases with decreasing L_D).

$$L_a = \left(2.4 \times 10^{-10}\right) \lambda_L^4 \left(\frac{A_D}{A_G}\right)^{-1} \tag{4}$$

$$L_D^2 = 1.8 \times 10^{-9} \lambda_L^4 \frac{A_G}{A_D} \tag{5}$$

The spectra shown in Fig. 10 indicate no significant difference between the virgin CF and the rCF. Determination of L_a and L_D for both samples indicates that the lateral cluster size L_a is slightly larger in the virgin CF ($L_a \approx 10$ nm) than in the recovered fibers ($L_a \approx 8.4$ nm), whereas L_D of the virgin CF (ca. 8 nm) was found to be significantly larger than that of the rCF (ca. 3.6 nm). Thus, the recovered samples rCF possess slightly lower crystallinity and an increased density of defects (i.e., a significantly lower inter-defect distance) as compared to the virgin CF. This may indeed correlate with the observed impact of the MSA exposure on the mechanical properties of the rCF.

4 Conclusion

In this study, CFRP recycling was conducted through the degradation of the epoxy resin with minimal damage to the CF. Among the three solvents tested, MSA, a non-oxidizing strong acid, exhibited the best performance, resulting in a

Table 6. Mechanical properties of virgin CF and rCF.

Recycled for	Ø max. breaking strength [GPa]	Standard deviation absolute	Ø elongation at breakage [%]	Standard deviation absolute	Ø max. elastic modulus [GPa]	Standard deviation absolute
0 h (virgin)	4.60	1.18	1.9	0.47	266	6.90
1 h	4.50	1.12	1.9	0.42	259.93	10.55
2 h	4.00	1.35	1.67	0.51	263	18.00
3 h	3.33	0.99	1.7	0.33	215	17.00

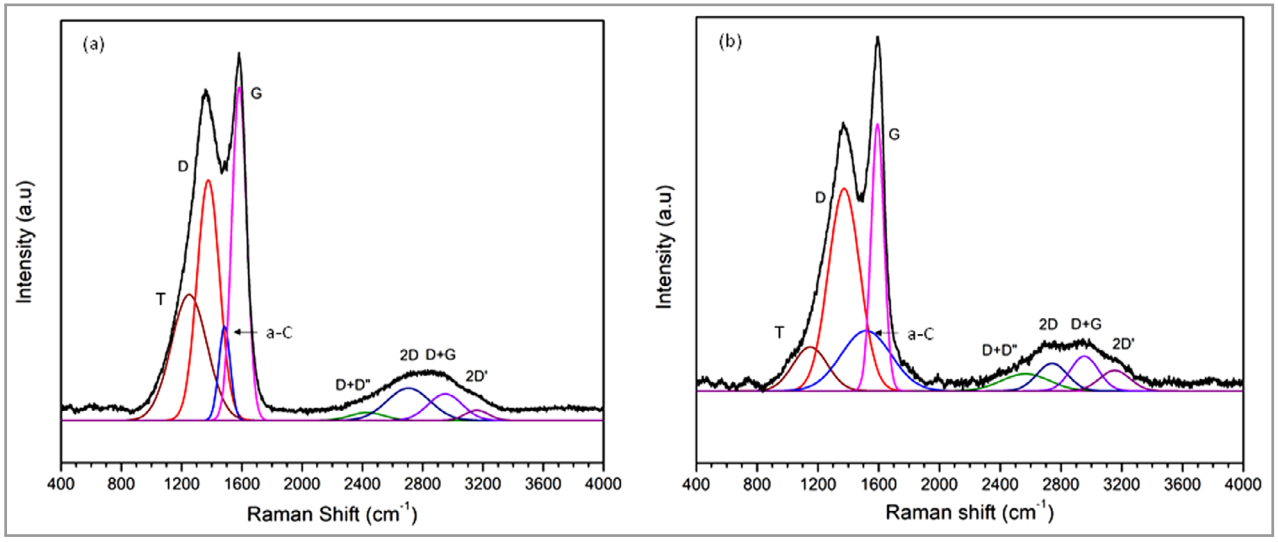

Figure 10. Raman spectra of (a) virgin CF and (b) rCF obtained after MSA exposure.

recycled epoxy yield of up to 89 wt %, compared to the original matrix content in CFRP. SEM analysis confirmed clean CF with the lowest residual epoxide levels (5 wt %). FTIR analysis revealed a decomposition mechanism involving selective carbon-nitrogen bond cleavage, leaving benzene rings and aromatic ethers (C—O—C) intact. Clearly, the strong Brønsted acid protonates the amine functions in the resin and makes them prone to cleavage. TGA and DSC measurements showed that the CFRP with a high-density crosslinked epoxy network underwent effective decomposition into polymer fragments and oligomers, with an earlier onset of degeneration (118 °C) and a reduction of more than 50 % in glass transition compared to virgin epoxy. The optimal solvolysis condition was identified as 100 % MSA for 2.5 h at 90 °C, with the decomposition of the resin almost completed within this timeframe. GPC measurements and single-fiber tests demonstrated a relatively narrow molecular distribution in the recycled epoxy after 2 h, with a slight reduction in mechanical properties after 3 h (28.3 % reduction in the maximum breaking strengths). Raman spectra analysis revealed slightly lower crystallinity and increased defect density in the recovered CF samples. In conclusion, a mild and effective chemical recycling method for CFRP waste was established, and the optimal solvolysis condition was determined. The successful recovery of CF and epoxy resin with good properties paves the way for their reuse in manufacturing, while future research is directed towards developing a catalytic version of the presented process.

Acknowledgments

The authors would like to thank Martina Heinz from the Institute of Technical Chemistry for carrying out the GPC measurements. We also thank Thomas Peter from the Institute of Non-Metallic Materials for the SEM and EDX measurements. Dharma T. Teja from the Institute of Materials Science, TU Darmstadt, is kindly acknowledged for recording and deconvoluting the Raman spectra of the carbon fiber samples.

This project is funded by the Deutsche Bundesstiftung Umwelt Project of Development of a resource-efficient production and recycling process for CFRP.

Open access funding enabled and organized by Projekt DEAL.

Symbol used

D	[–]	dispersity
D_d	[wt %]	degradation degree
L_a	[nm]	lateral cluster size
L_D	[nm]	inter-defect distance
T_g	[°C]	glass transition temperature
W	[kg]	weight

Sub-/superscripts

v	virgin
r	recovered
f	fiber
m	matrix
c	composites
rc	recovered composites
rm	recovered matrix
rf	recovered fiber

Abbreviations

CF	carbon fiber
CFRP	carbon fiber-reinforced plastics
DGEBA	bisphenol A diglycidyl ether
FTIR	Fourier transform infrared
DSC	differential scanning calorimetry
FVC	calculated fiber volume fraction
GPC	gel permeation chromatography
HDDGE	1,6-hexanediol diglycidyl ether
IPDA	isophorone diamine
MSA	methanesulfonic acid
MWD	molecular weight distribution
PDI	polydispersity index
SEM	scanning electron microscopy
TGA	thermogravimetric analysis
VARI	vacuum-assisted resin infusion

References

[1] J. P. Jensen, *Wind Energy* **2019**, *22* (*2*), 316–326. DOI: https://doi.org/10.1002/we.2287

[2] M.-A. Dupré la Tour, *Renewable Sustainable Energy Rev.* **2023**, *179*, 113189. DOI: https://doi.org/10.1016/j.rser.2023.113189

[3] B. K. Sovacool, M. A. M. Perea, A. V. Matamoros, P. Enevoldsen, *Wind Energy* **2016**, *19* (*9*), 1623–1647. DOI: https://doi.org/10.1002/we.1941

[4] D. S. Cousins Y. Suzuki, R. E. Murray, et al., *J. Cleaner Prod.* **2019**, *209*, 1252–1263. DOI: https://doi.org/10.1016/j.jclepro.2018.10.286

[5] L. Mishnaevsky, K. Branner, H. Nørgaard Petersen, et al., *Materials (Basel)* **2017**, *10* (*11*), 1285. DOI: https://doi.org/10.3390/ma10111285

[6] G. Oliveux, L. O. Dandy, G. A. Leeke, *Prog. Mater. Sci.* **2015**, *72*, 61–99. DOI: https://doi.org/10.1016/j.pmatsci.2015.01.004

[7] M. Rani, P. Choudhary, V. Krishnan, S. Zafar, *Composites, Part B* **2021**, *215*, 108768. DOI: https://doi.org/10.1016/j.compositesb.2021.108768

[8] K. Anane-Fenin, E. T. Akinlabi, E. T. Akinlabi, in *Proceedings of the DII-2017 Conference on Infrastructure Development and Investment Strategies for Africa*, Livingstone **2017**.

[9] F. Petrakli, A. Gkika, A. Bonou, et al., *Polymers (Basel)* **2020**, *12* (*9*), 22. DOI: https://doi.org/10.3390/polym12092129

[10] X. Xue, S.-Y. Liu, Z.-Y. Zhang, et al., *J. Reinf. Plast. Compos.* **2022**, *41* (*11/12*), 459–480. DOI: https://doi.org/10.1177/07316844211055208

[11] L. Wang, R. Templer, R. J. Murphy, *Bioresour. Technol.* **2012**, *120*, 89–98. DOI: https://doi.org/10.1016/j.biortech.2012.05.130

[12] A. Villanueva, H. Wenzel, *Waste Manage.* **2007**, *27* (*8*), S29–S46. DOI: https://doi.org/10.1016/j.wasman.2007.02.019

[13] J. R. Correia, N. M. Almeida, J. R. Figueira, *J. Cleaner Prod.* **2011**, *19* (*15*), 1745–1753. DOI: https://doi.org/10.1016/j.jclepro.2011.05.018

[14] S. Agterbosch, W. Vermeulen, P. Glasbergen, *Energy Policy* **2004**, *32* (*18*), 2049–2066. DOI: https://doi.org/10.1016/S0301-4215(03)00180-0

[15] N. Kanari, J. L. Pineau, S. Shallari, *JOM* **2003**, *55* (*8*), 15–19. DOI: https://doi.org/10.1007/s11837-003-0098-7

[16] A. van Schaik, M. A. Reuter, *JOM* **2004**, *56* (*8*), 39–43. DOI: https://doi.org/10.1007/s11837-004-0180-9

[17] S. Pimenta, S. T. Pinho, *Waste Manage.* **2011**, *31* (*2*), 378–392. DOI: https://doi.org/10.1016/j.wasman.2010.09.019

[18] S. S. Yao, F. L. Jin, K. Y. Rhee, et al., *Composites, Part B* **2018**, *142*, 241–250. DOI: https://doi.org/10.1016/j.compositesb.2017.12.007

[19] A. Torres, I. de Marco, B. M. Caballero, et al., *Fuel* **2000**, *79* (*8*), 897–902. DOI: https://doi.org/10.1016/S0016-2361(99)00220-3

[20] R. L. Perez, C. E. Ayala, M. M. Opiri, et al., *ACS Appl. Polym. Mater.* **2021**, *3* (*11*), 5588–5595. DOI: https://doi.org/10.1021/acsapm.1c00896

[21] J. H. Ma, X. B. Wang, B. Li, L. N. Huang, *Adv. Mater. Res.* **2009**, *79*, 409–412.

[22] W. Ballout, N. Sallem-Idrissi, M. Sclavons, et al., *Sci. Rep.* **2022**, *12* (*1*), 5928. DOI: https://doi.org/10.1038/s41598-022-09932-0

[23] Y. J. Ma, D. Kim, S. R. Nutt, *Polym. Degrad. Stabil.* **2017**, *146*, 240–249. DOI: https://doi.org/10.1016/j.polymdegradstab.2017.10.014

[24] T. Hanaoka, Y. Arao, Y. Kayaki, et al., *Polym. Degrad. Stabil.* **2021**, *186*, 109537. DOI: https://doi.org/10.1016/j.polymdegradstab.2021.109537

[25] T. Hanaoka, H. Ikematsu, S. Takahashi, et al., *Composites, Part B* **2022**, *231*, 109560. DOI: https://doi.org/10.1016/j.compositesb.2021.109560

[26] C. Ma, D. Sánchez-Rodríguez, T. Kamo, *Polym. Degrad. Stabil.* **2020**, *178*, 109199. DOI: https://doi.org/10.1016/j.polymdegradstab.2020.109199

[27] T. S. Deng, Y. Liu, X. Cui, et al., *Green Chem.* **2015**, *17* (*4*), 2141–2145. DOI: https://doi.org/10.1039/c4gc02512a

[28] K. Li, Z. Xu, *Environ. Sci. Technol.* **2015**, *49* (*3*), 1761–1767. DOI: https://doi.org/10.1021/es504644b

[29] X. Y. Gong, H. J. Kang, Y. Y. Liu, S. Q. Wu, *RSC Adv.* **2015**, *5* (*50*), 40269–40282. DOI: https://doi.org/10.1039/c5ra03828f

[30] Y. Y. Liu, H. Kang, X. Gong, et al., *RSC Adv.* **2014**, *4* (*43*), 22367–22373. DOI: https://doi.org/10.1039/c4ra02023e

[31] M. F. Xing, F. S. Zhang, *Chem. Eng. J.* **2013**, *219*, 131–136. DOI: https://doi.org/10.1016/j.cej.2012.12.066

[32] I. Okajima, M. Hiramatsu, Y. Shimamura, et al., *J. Supercrit. Fluids* **2014**, *91*, 68–76. DOI: https://doi.org/10.1016/j.supflu.2014.04.011

[33] H. Yan, C. X. Lu, D. Q. Jing, X. L. Hou, *Polym. Degrad. Stabil.* **2013**, *98* (*12*), 2571–2582. DOI: https://doi.org/10.1016/j.polymdegradstab.2013.09.026
[34] G. Jiang, S. J. Pickering, E. H. Lester, et al., *Compos. Sci. Technol.* **2009**, *69* (*2*), 192–198. DOI: https://doi.org/10.1016/j.compscitech.2008.10.007
[35] P. L. Xu, J. Li, J. P. Ding, *Compos. Sci. Technol.* **2013**, *82*, 54–59. DOI: https://doi.org/10.1016/j.compscitech.2013.04.002
[36] T. Liu, M. Zhang, X. Guo, et al., *Polym. Degrad. Stabil.* **2017**, *139*, 20–27. DOI: https://doi.org/10.1016/j.polymdegradstab.2017.03.017
[37] T. Iwaya, S. Tokuno, M. Sasaki, et al., *J. Mater. Sci.* **2008**, *43* (*7*), 2452–2456. DOI: https://doi.org/10.1007/s10853-007-2017-8
[38] J. Britschgi, W. Kersten, S. R. Waldvogel, F. Schuth, *Angew. Chem. Int. Ed. Engl.* **2022**, *61* (*41*), e202209591. DOI: https://doi.org/10.1002/anie.202209591
[39] F. C. Walsh, C. P. de León, *Surf. Coat. Technol.* **2014**, *259*, 676–697. DOI: https://doi.org/10.1016/j.surfcoat.2014.10.010
[40] N. Pewnim, S. Roy, *Electrochim. Acta* **2013**, *90*, 498–506. DOI: https://doi.org/10.1016/j.electacta.2012.12.053
[41] M. D. Gernon, M. Wu, T. Buszta, P. Janney, *Green Chem.* **1999**, *1* (*3*), 127–140. DOI: https://doi.org/10.1039/a900157c
[42] J. A. J. Wang, F. Ren, T. Tan, J. Mandell, Oak Ridge National Laboratory, Oak Ridge, Tennessee **2010**.
[43] M. R. Acocella, C. Esposito Corcione, A. Giuri, et al., *RSC Adv.* **2016**, *6* (*28*), 23858–23865. DOI: https://doi.org/10.1039/c6ra00485g
[44] M. Gebhardt, I. Manolakis, G. Kalinka, et al., *Compos. Commun.* **2021**, *28*, 100974. DOI: https://doi.org/10.1016/j.coco.2021.100974
[45] EPIKOTE Resin MGS, Technical Data Sheet [Print] **2006**.
[46] L. Saini, N. S. Sankar, R. Aparna, et al., *Nat. Commun.* **2022**, *13* (*1*), 498. DOI: https://doi.org/10.1038/s41467-022-28162-6
[47] A. C. Ferrari, J. Robertson, *Philos. Trans. R. Soc., A* **2004**, *362* (*1824*), 2477–2512. DOI: https://doi.org/10.1098/rsta.2004.1452
[48] L. G. Cançado, K. Takai, T. Enoki, et al., *Appl. Phys. Lett.* **2006**, *88* (*16*), 163106. DOI: https://doi.org/10.1063/1.2196057
[49] L. G. Cancado, A. Jorio, E. H. Martins Ferreira, et al., *Nano Lett.* **2011**, *11* (*8*), 3190–3196. DOI: https://doi.org/10.1021/nl201432g

